Pull-out of backfill geogrid reinforcement for retaining walls

D.V. Reddy, S. Gao
Florida Atlantic University, Boca Raton, Florida, U.S.A.

F. Navarrete
Florida Atlantic University, Boca Raton, Florida, U.S.A.

Consejo Nacional de Ciencia y Tecnologia, Mexico, D.F. Mexico

P. Lai
Florida Department of Transportation (FDOT), Tallahassee, Florida, U.S.A.

Keywords: Geogrids, Pull-out, Reinforcement, Walls

ABSTRACT: This study addresses the long term pullout resistance carried out for two types of geogrids: HDPE and PET. Sand and limerock are used for the backfill material, with simulation of unsaturated and saturated conditions. Eight pullout test boxes were designed and constructed each with a specially designed stainless steel clamps. The measured strain-time relations for unsaturated and saturated soils for various levels of the pullout force until the peak value (up to 10,000 hours of exposure), and varying distances from the loading end were plotted. The analytical simulation was by finite elements. The soil was modeled using conventional solid elements that are eight-noded isoparametric elements, and reinforcement with flexible beam elements. The experimental values were compared with some of the analytical ones. The normal and principal stresses in the soil, and the strains along the geogrid were determined from the finite element analysis for the unsaturated soil condition for various pullout force levels. There were significant reductions in the pullout resistance in saturated soil for the HDPE and PET geogrids. The results were analyzed, and a generalized method proposed for practical design using sliding resistance factors.

1 INTRODUCTION

Due to the economic advantages, the use of polymeric reinforcement in soil-reinforced structures has increased considerably. With the rapid development of the geosynthetic industry, there is a wide range of applications for geogrid reinforcement in soil, such as retaining walls, embankments, paved roads, foundations, and slope stabilization.

Geogrids are matrix-like materials with large open spaces , which are typically 10 to 100 mm between ribs. The primary function of geogrids is clearly reinforcement. Koerner (1998). The bonding between soil and reinforcement creates a more efficient, cost-effective structure.

However, due to the relatively short experience with these polymeric materials, there are uncertainties regarding their durability, with respect to retainment of the design properties after being subjected to construction stresses and exposed to in-soil environments over the expected design life. Potential degradation of polymeric reinforcement, with time, will depend on the characteristics of a specific polymer, configuration, and the environment to which it is exposed. This dictates the need for more research in this area. If geogrids have to be used as an alternative to steel reinforcement to overcome the corrosion problem, their performance has to be established based on laboratory and field testing for site specific conditions, e.g. high water tables and temperatures ranging between 27° C to 38° C in Florida. Typical soil temperatures are in the range of 10° C to 16° C; temperatures near the surface of the wall can reach 29° C to 38° C. The pH values

of various MSE materials used by the Florida Department of Transportation are in the range of 4.5 to 9.

1.1 *HDPE Geogrids*

HDPE is the acronym for High Density Polyethylene, The uniaxial HDPE geogrids used in this research are manufactured by stretching a punched sheet of extruded HDPE in one direction, under carefully controlled conditions. This process aligns the polymer's long-chain molecules in the direction of drawing, and results in a product with high one-directional tensile strength and modulus.

1.2 *PET Geogrids*

PET is the acronym for Polyester Terephthalate. PET geogrids are made of polyester multifilament yarns, which are interlocked by weaving to create a stable network, such that the yarns retain their relative position. Compared to HDPE, PET is more flexible in bending and exhibits a relatively lower junction strength.

1.3 *Pull-out*

Stresses in the reinforcing elements are transferred to the surrounding soil by bonding between the soil and the reinforcement. This bond is formed through 1) friction, 2) passive soil resistance, or 3) a combination of both, and developed along both sides of the reinforcing element in the resisting zone behind the failure plane. To maintain equilibrium, the bond must resist the maximum tensile load carried by the reinforcing element (pullout resistance).

Pullout resistance of geosynthetics is one aspect of analysis that relates both designs of reinforced soil structures such as walls and slopes and the configuration of any anchor trench in a geomembrane-lined containment facility. Factors influencing the evaluation of pullout resistance in the laboratory are the type of soil, material properties, including coating, geometry of the geosynthetic, and the test apparatus Fannin and Raju (1991). Soil parameters of major interest are the shear strength characteristics, effective stress, and coefficient of frictional interaction. Since pullout resistance is a function of soil-geosynthetic interaction, the tensile strength, and geometric shape of the geogrid are of major importance. The test setup, depends on the sample dimensions, boundary conditions, and the loading system.

Factors affecting the evaluation of pullout resistance are the type of soil, material properties, geometry of the geosynthetic, and configuration of the test apparatus. The last factor, namely configuration of the test apparatus, relates to the sample dimensions and its preparation, boundary conditions, and the loading system Fannin *et al*. (1994).

2 EXPERIMENTAL INVESTIGATION

2.1 *Test procedures*

Eight pullout boxes were designed at Florida Atlantic University (1996) to evaluate the development of pullout resistance with increasing displacement of the geogrid specimens. Measurements included pullout force, pullout displacement, and strain in the geogrid specimens, Figures 1 and 2.

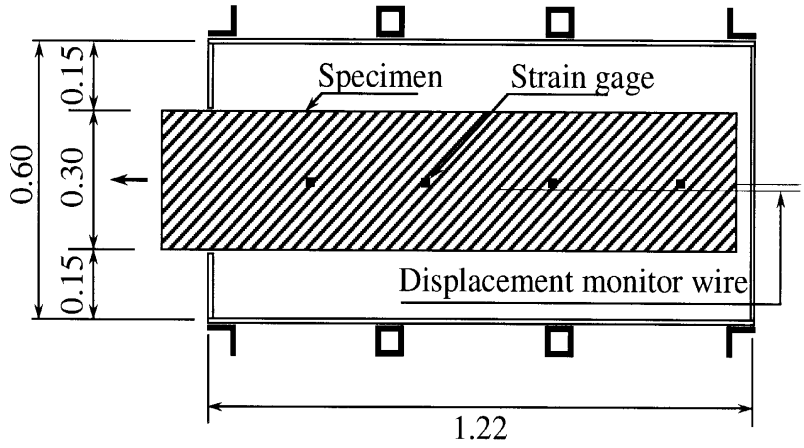

Figure 1. Plan of pullout box

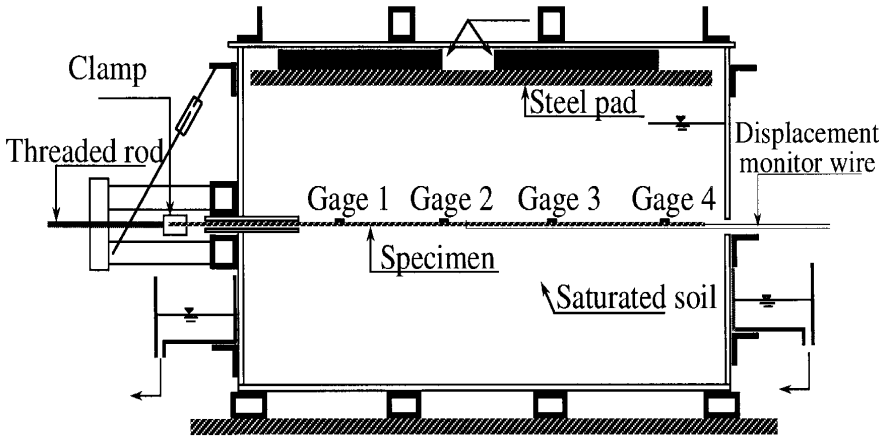

Figure 2. Longitudinal section of pullout box

The pullout box contained the soil sample and geogrid test specimen with a clamp assembly for gripping the geogrid test specimen, airbags for imposing confining pressure, a spring assembly for the application of the pullout force, and a watering system for the saturated condition.

The eight boxes had the following combinations:

Test 1: HDPE in limerock under saturated condition
Test 2: PET in limerock under saturated condition
Test 3: HDPE in sand under saturated condition
Test 4: PET in sand under saturated condition
Test 5: HDPE in sand under unsaturated condition
Test 6: PET in sand under unsaturated condition
Test 7: HDPE in limerock under unsaturated condition
Test 8: PET in limerock under unsaturated condition

Four strain gages were fixed on each test specimen to measure tensile strains during the testing. Their location was along the center line of the specimen with 250 mm spacing (Figures 1 and 2).

The surface of the last layer of sand (limerock) was leveled to receive the built-up steel pad. This pad was made of two steel plates and eight box stiffeners. It was rigid enough to distribute the

surcharge load uniformly. The top level of the load plate was at the same level as the rim of the pullout box. The confining pressure was about 41 kPa.
For the tests under saturated condition, water was filled in slowly from the inlet on the top of the pullout box. The water level was checked through a plastic hose from the bottom of the box. When the water reached the level at the top of the exit slot, water filling was stopped. Any surplus water was collected by water collectors located at both ends of the pullout box, and drained into the sewer through another set of plastic tubes.

2.2 *Test results*

The results are presented for pullout tests on both HDPE and PET test specimens. The test conditions addressed saturated and unsaturated soil. The confining pressure was kept at about 41 kPa at the geogrid specimen level. The test mode was in load-control. In each test, a sustained load was applied incrementally until the specimen was pulled out. The first loading stage (Stage-I) was kept for about 9,800 hours under 10% of expected pullout load. In the second loading stage (Stage-II), a sustained load of 10 to 25% of the expected pullout load was applied incrementally. Each increment lasted for approximately 25 hours.

The peak pullout resistance occurred when the displacement of the embedded end was first observed. Any larger pullout load would be accompanied with substantial displacement and a quick drop back.

Figures 3 and 4 show the strain-time relation for the eight pullout tests at the first testing stage (Stage-I) based on gage readings in gage 1. The pullout load was 4.27 kN/m for the tests under the saturated test condition, and 5.693 kN/m for tests under the unsaturated condition. These loads had been maintained for about 9,800 hours. As this was the initial load application stage (Stage-I), the geogrid specimen experienced an unstable stage in which some degree of sliding occurred. It is a natural phenomenon when the geogrid specimens are initially pulled.

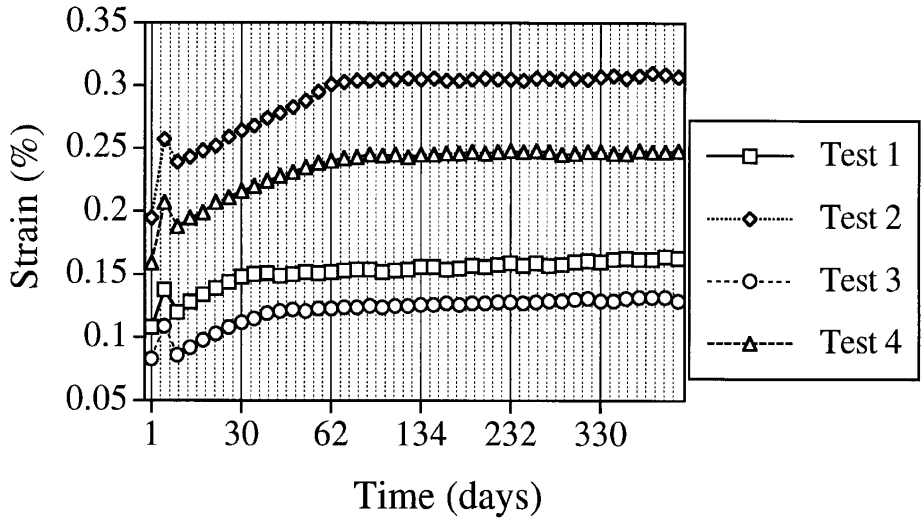

Figure 3. Strain-time relations for HDPE and PET geogrids in sand and limerock under saturated condition at stage-I (strain gage 1)

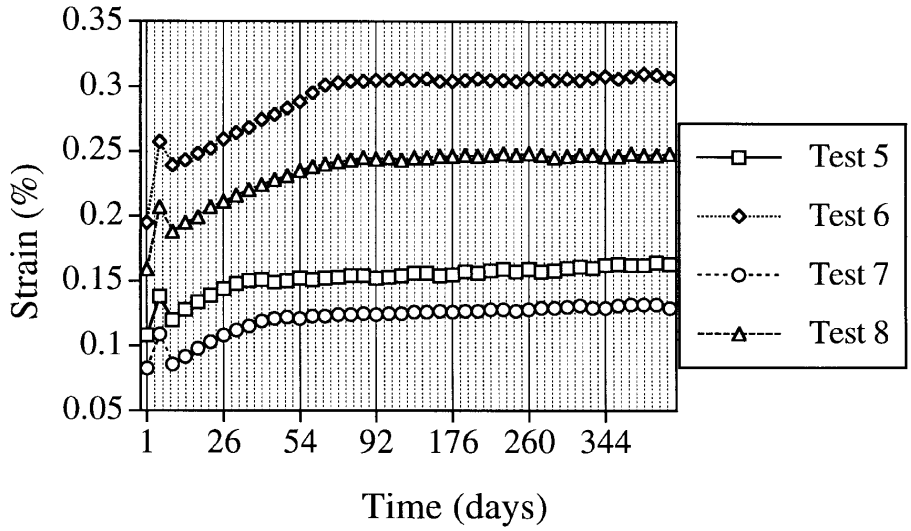

Figure 4. Strain-time relations for HDPE and PET geogrids in sand and limerock under saturated condition at stage-I (strain gage 1)

Figures 5 and 6 are two of the figures that represent the final pullout stage (Stage-II) of the tests. In each test, the pullout load was applied incrementally until the specimen was pulled out. For tests under saturated condition, the first four pullout loading steps were 11.39 kN/m, 21.35 kN/m, 31.31 kN/m, and 35.58 kN/m. For tests under unsaturated condition, the first four pullout loading steps were 15.66 kN/m, 31.31 kN/m, 45.55 kN/m, and 54.09 kN/m. The peak value of the pullout load was different for each test, depending on the calculated peak capacity. Each load increment was maintained constant for about 25 hours. The increment was about 10 to 25% of the expected pull-out load. The geogrid anchorage capacity was defined as the pullout load at which the embedded end of the geogrid specimen started to move.

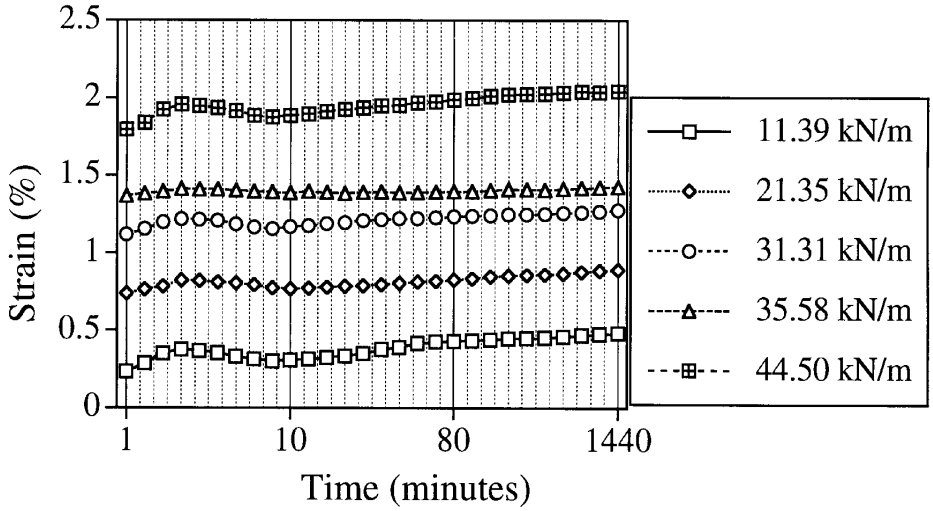

Figure 5. Strain-time relations for HDPE geogrid in limerock under saturated condition at stage-II (strain gage 1)

From the test results, it was observed that the characteristic response of the curve can be divided into four zones, an initial strain increasing soon after the application of the pullout force, an unstable zone with some drop in the strain value, a transition zone with gradual strain increment, and a final stable zone.

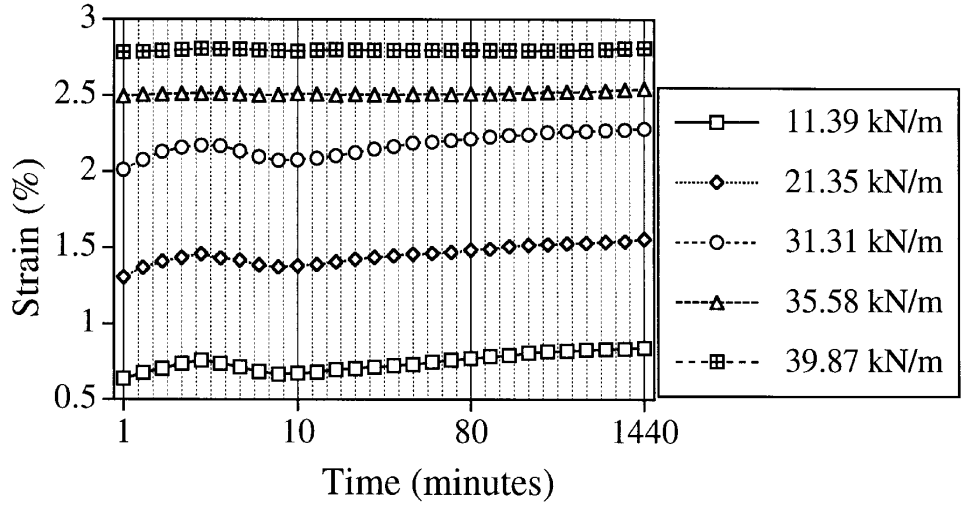

Figure 6. Strain-time relations for PET geogrid in limerock under saturated condition at stage-II (strain gage 1)

Figures 7 and 8 show the strain distribution profiles along the specimens based on the distance from the front wall. The strain readings are from gages 1, 2, 3, and 4. The load level was at the final pullout loading stage (Stage II).

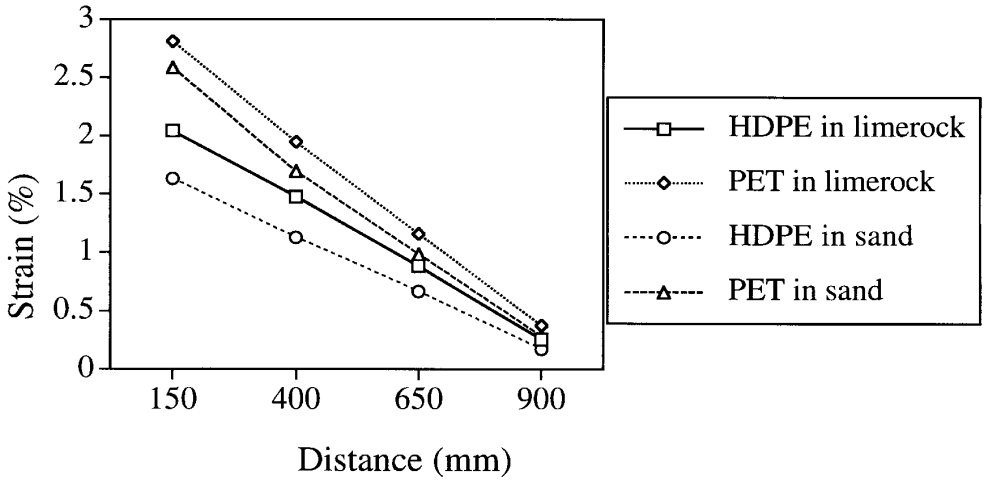

Figure 7. Strain distributions with respect to the distance from the front wall for HDPE and PET geogrids in limerock under saturated condition at P_{ult}.

For the strain distribution pattern along the test specimen, a similar trend and contours can be seen clearly. In each case, the strain decreases with the distance from the clamped end, and the magnitude of the strain at the front end was greater than that at the rear end. Compared to the strain at the front end, the strain at the rear end is about six to nine times smaller. This is because the interface resistance between the soil and geogrid prevents the pullout load very effectively from being transmitted to the rear part of the geogrid specimen.

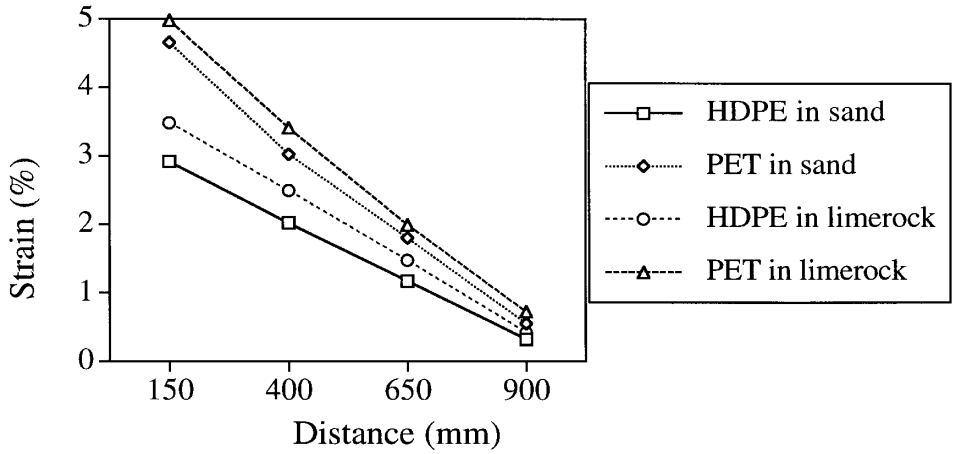

Figure 8. Strain distributions with respect to the distance from the front wall for HDPE and PET geogrids in limerock under unsaturated condition at P_{ult}.

2.3 *Finite element analysis*

The pullout test for unsaturated soil condition was simulated by the finite element method (Software: ANSYS 5.3) in analyzing the reinforced solid soils. The uniformly distributed load was applied on the top of the soil element to simulate the confining pressure. The boundary conditions of the front and back walls are roller-supported conditions between soil and side walls. The bottom nodes were fully restrained in all three directions.

The soil elements and the reinforcing elements were modeled by using eight-noded isoparametric elements. This element is defined by eight nodes with two degrees of freedom at each node: translations in the nodal x and y directions. It has plasticity, creep, swelling, stress, stress stiffening, large deflection, and large strain capabilities.

The interface element was modeled by contact elements. This element represents two surfaces that may be continuous or break or slide relative to each other. It has the capacity of supporting compression in the direction normal to the surfaces and shear in the tangential direction. The element has two degrees of freedom at each node: translations in the x and y direction. The geometry, node locations, and the coordinate system for this element are shown in Figures 9.

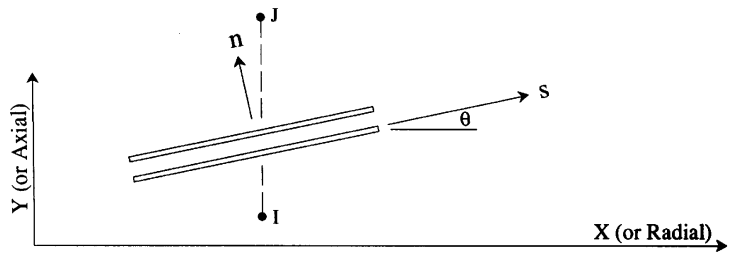

Figure 9. Interface Element

The confining pressure was applied and kept constant on the top of soil specimen, while the pullout load acting on the reinforcing element was increased step by step, until the peak value was reached. During this process, the pullout force is applied according to some percentage of the total pullout load. These are 10%, 25%, 50%, 75%, and 90%.

This enables the monitoring of stress and strain during the pullout force application. When the pullout force reached 100% of pullout load, failure occurred, no measurements could be made.

The principal stress distribution was very uniform throughout the test modeling under the confining pressure only. The application of pullout force interrupted this uniformity. When the pullout force at 10% of total pullout load, the stress variation was very little. It extended to only 70 mm from the front wall. The high stress variation area extended further to the back, as far as 200 mm, when the pullout force reached 25% of total pullout load. The affected range in the vertical direction was 50 mm above and below the reinforcement. As the pullout force reaches 50% of total pullout load, the large variation area kept moving toward the back wall, with the furthest end as far as 550 mm from the front wall, and well beyond the vertical centerline of the test setup. The effective range in the vertical direction was 100 mm.

Under the 75% of total pullout load, the high stress variation area kept propagating backward, extending to about 80% of the total length of the reinforcing element. At the sub-final loading stage (90% of total pullout load), the stress concentration area extended almost through all the length of the model, finally reaching the rear wall. This means that almost the whole zone surrounding the reinforcing element was under critical condition, and pullout failure was imminent. At the final loading stage (100% of total pullout load), the last contact element at the very rear end of the model failed. The whole reinforcement element slided out of the pullout setup, the deformation was larger than the software's display-limit .

The strain variations obtained with the ANSYS 5.3 occurred mainly in the reinforcing elements. The strain variations in the soil element were very limited and unnoticeable compared to those in the reinforcing element. There are two major reasons for this phenomenon. Firstly, the soil element was restrained within the pullout box; the roller boundary condition did not allow any movement horizontally, especially in the regions near the front and rear ends of the reinforcing elements. Secondly, the pullout load was applied directly on the reinforcing element, not on the soil elements.

Figure 10 shows that the results from the experimental investigation and the finite element analysis, for the unsaturated soil test condition, are in good agreement.

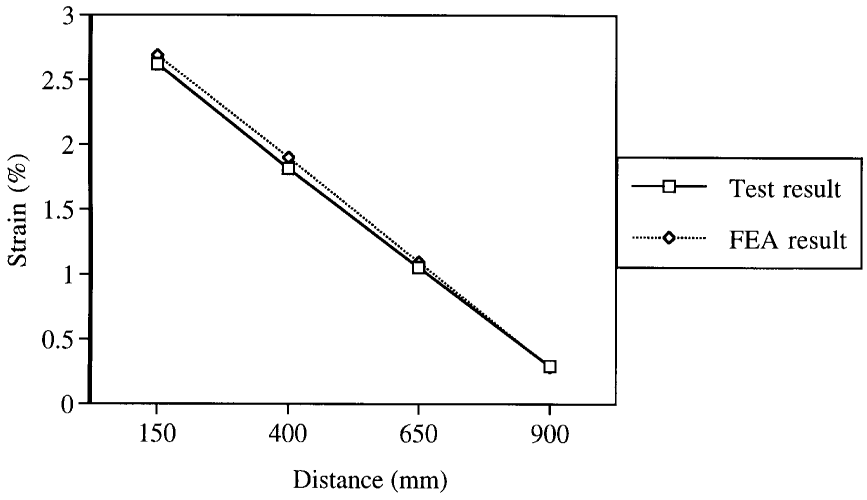

Figure 10. Observed and calculated strain distributions for a HDPE geogrid in sand under unsaturated condition

The strains at the front end were about eight times higher than those at the rear end. This shows that the friction developed between the reinforcing element and the soil, and the bearing, can very effectively prevent the pullout force from transmitting. Both HDPE and PET are very good materials for geogrid soil reinforcement. However, there is an identified need to analytically predict the pullout strength for saturated soil conditions.

2.4 *Practical design applications*

For the reinforced earth design, the sliding coefficient is very dependent on the type of geogrid, the spacing of layers, and the length of the reinforcement. In the reinforced soil slope design (Figures 11 and 12), the bond length required is critical to mobilize the allowable design strength. Both the sliding coefficient and the bond length required are based on the data from the pullout testing.

The ultimate pullout load must be less than or equal to the allowable long-term pullout design load. The safety factor of 1.5, recommended by The Federal Highway Administration (FHWA), USA, was applied to the design bond length . For reinforced soil slope and embankment applications, the strains are not the controlling factor but the bond length. These types of structures can tolerate a larger deformation and more movement. The geogrid PET is a very good choice for these applications because of low cost and easy handling and high resistance to creep and creep rupture.

In reinforced earth wall design, the deformation and displacement control are very important for the structure performance. The limiting strain becomes the critical design factor. For design applications, greater density of reinforcement is highly recommended for both geogrids HDPE and PET, and it is important to evaluate and verify the resistance factors for creep, durability, and construction damage.

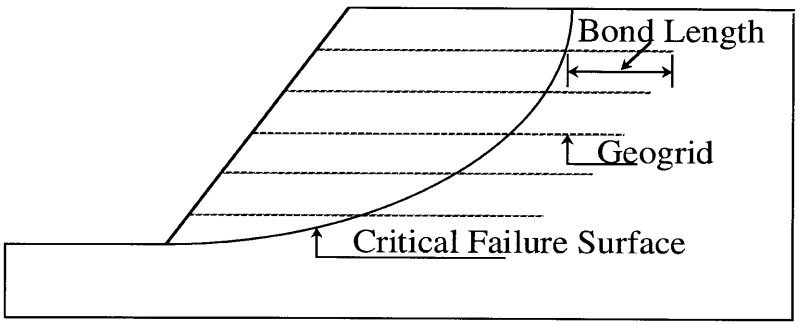

Figure 11. Design controlled by bond length

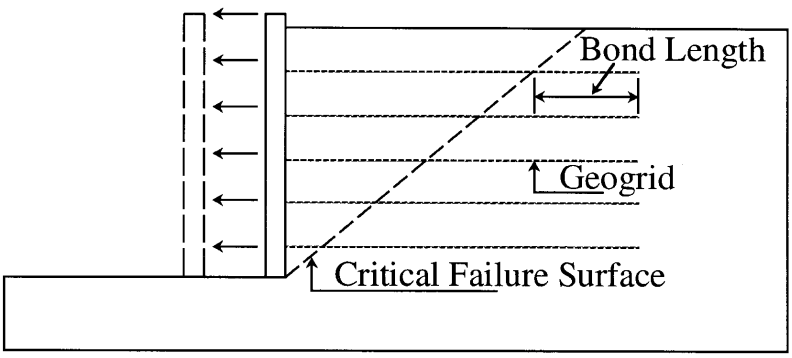

Figure 12. Design controlled by deformation

3 CONCLUSIONS

Under unsaturated working conditions, the geogrid HDPE has a sliding coefficient of 1.05 in coarser soil with good gradation, compared to 1.02 for the finer sand specimen. In contrast for the PET geogrid, the sliding coefficient in coarser soil condition was 1.08, but for the finer soil condition, the sliding coefficient increased to 1.12.

Based on the tests and theoretical analysis, the PET geogrid has better pullout resistance performance than the HDPE geogrid, when used in fine sand (sliding coefficient is 1.12 under unsaturated working condition). Since fine sand can provide more contact surface, a larger friction resistance is mobilized. On the other hand, for the HDPE geogrid, a coarser sand with good gradation is the better choice (sliding coefficient is 1.05 under unsaturated working condition).

For a PET geogrid in limerock, the sliding coefficient was 1.08 under the unsaturated testing condition, and 0.669 under the saturated condition. This gives a 38.1% reduction due to the wetting effect. Similarly, the sliding coefficient for test specimen PET in sand was 1.12 in the unsaturated condition, and 0.688 under saturated condition. From the test results, it can be inferred that the wetting condition causes a 38.6% decrease in the resistance.

For the test specimen HDPE in limerock, the sliding coefficient was 1.05 in the unsaturated condition and 0.758 under the saturated condition. The decrease was only 27.8%. In sand, the sliding coefficient was 1.02 under the unsaturated condition, and 0.729 under the saturated condition, with a 28.5% reduction.

From the test results, it can be inferred that the saturated condition has more impact on fine sand than coarser sand; the reduction in the sliding coefficient is larger for the PET geogrid than the HDPE geogrid. This is because the friction resistance is subjected to a greater loss due to saturation, and the bearing resistance is marginal.

ACKNOWLEDGEMENTS

This paper is based on a Florida Department of transportation (FDOT) funded project entitled "Strength and Durability of Backfill Geogrid for Retaining Walls", Work Program # 0510738. The authors are grateful to FDOT for the funding. The support and encouragement of Dr. S.E. Dunn, Professor and Chairman of the Department of Ocean Engineering, and Dr. J.T. Jurewicz, Dean of Engineering, are gratefully acknowledged. Thanks are also due to Consejo Nacional de Ceiencia y Tecnologia (CONACYT) for its support to the second author F. Navarrete.

REFERENCES

Fannin, R. J., Hermann, S., Vaslestad, J., and Raju, D. M. 1994. Coefficients of Interface Bond in Reinforced Soil Structures, *Proceedings of the 13th International Conference on Soil Mechanics and Foundation Engineering*, New Delhi, India.

Fannin, R. J., and Raju, D. M. 1991. Pullout Resistance of Goesynthetics, *Proceedings of the 44th Canadian Geotechnical Conference*, Calgary, Vol. 2.

Gao, S. 1998. Long-Term Pullout Resistance of Geogrid Reinforcement for Retaining Walls, *Master Thesis*, Florida Atlantic University, Boca Raton, Supervisor: Dr. Reddy, D.V., Florida DOT Research Contract Monitor: Lai P.

Koerner, M. R. 1998. 4th ed. *Designing With Geosynthetics*. Upper Saddle River, NJ, USA.Prentice Hall,

Reddy, D. V. 2000. Strength and Durability of Backfill Geogrid Reinforcement for Retaining Walls, *Report to FDOT*, Florida Atlantic University, Boca Raton, FL, USA.